

Calculation of the temperature integrals used in the processing of thermogravimetric analysis data

INGENIERIA QUIMICA

Cálculo de las integrales de temperatura usadas en el procesamiento de datos de análisis termogravimétrico

J. I. Carrero-Mantilla^{1§}, A. F. Rojas-González¹

Universidad Nacional de Colombia, Faculty of Engineering, Chemical Engineering Department, Manizales, Colombia¹

§jicarrerom@unal.edu.co, anfrojasgo@unal.edu.co

(Recibido: 02 de Febrero de 2019 – Aceptado: 04 de Junio de 2019)

Abstract

There is no standard procedure for calculating the generalized temperature integral, instead myriads of different approximations to it are applied in the processing of thermogravimetric analysis data. This work presents first an integration procedure based on the Simpson rule that generates reference values of the generalized temperature integral. It also reviews the available representations of the temperature integral in power series, and presents the conversion of its generalized form into the form of special functions. From the comparison with the reference values from integration it was concluded that for argument values of practical interest the generalized temperature integral is best computed as the incomplete gamma function.

Keywords: *Incomplete gamma function, Temperature integral, Thermogravimetric analysis.*

Resumen

No hay un procedimiento normalizado para calcular la integral de temperatura generalizada, en lugar de eso, cantidades de aproximaciones distintas de ella son aplicadas en el procesamiento de datos de análisis termogravimétrico. Este trabajo presenta primero un procedimiento de integración basado en la regla de Simpson que genera valores de referencia de la integral de temperatura generalizada. También se realiza una revisión de las representaciones en series de potencias disponibles para la integral de temperatura, y se presenta la conversión de su forma generalizada a la forma de las funciones especiales. De la comparación con los valores de referencia obtenidos por integración se concluyó que, para valores de interés práctico de los argumentos, el mejor cálculo de la integral generalizada de temperatura se obtiene con la función gama incompleta.

Palabras clave: *Análisis termogravimétrico, Función gama incompleta, Integral de temperatura.*

1. Introduction

The temperature integral (Equation 1) is,

$$p(x) = \int_x^{\infty} \chi^2 \exp(-\chi) d\chi \quad (1)$$

(also named Arrhenius integral) is used in many non-linear analysis regression methods of thermogravimetric data as the solution of the differential equation that represents the variation in time of the fractional extent of conversion, or its integration between consecutive values ⁽¹⁻³⁾. In the field of thermal analysis most integral results are based on some approximate representation of $p(x)$ (general-purpose mathematical software, for example spreadsheets, do not include the temperature integral). But despite their prevalence in thermal analysis these approximations are in fact not necessary: $p(x)$ and its generalized form $p_m(x)$ can be calculated with specific series representations, and more importantly they can be rewritten in terms of the special functions ⁽⁴⁾.

Thermogravimetric analysis (TGA) has become a common technique for chemisorption, thermal decomposition, and solid-gas reactions. For the most part analysis of thermogravimetric data is settled in the ICTAC Kinetics Committee recommendations ^(5,6); but it is still an active research area and new methods have appeared after the ICTAC publications ⁽⁷⁻⁹⁾. There are also some aspects of TGA data analysis, such as heat inertia, still under development ^(10,11); while some others, like the use of logistic equation have been criticized ⁽¹²⁾. In our previous work both the prevalence of the linear regression and the use of approximations to $p(x)$ were rebutted developing a non-linear regression method for thermal analysis data based on the general form of the temperature integral ⁽⁴⁾.

In this explanatory work we focus solely on the calculation of $p_m(x)$ with special functions, starting with the development of a rigorous integration method to obtain benchmark values of the temperature integral for any value of m or x . This required two related tasks explained in Section 3, first a tiny stepsize was chosen minimizing the error associated to the integration method; and second, and an algorithmic equivalent of the infinity upper limit was established. Next, in Section 4, an overview of available direct representations of $p(x)$ in power series is presented followed by the transformation of $p_m(x)$ into special functions. Finally, the choice of the incomplete gamma function (Γ) is justified by comparisons against the numerical integration results. This conclusion is relevant not only for data analysis but also for the testing or calibration of the software built in, or included with, TGA instruments which is proprietary and tends to operate as a black box.

2. Generalization of the temperature integral

In thermal kinetics the fractional extent of conversion (α) is usually written as the product of the Arrhenius rate constant and a kinetic function f (Equation 2):

$$\frac{d\alpha}{dt} = A \exp\left(-\frac{E}{RT}\right) f(\alpha) \quad (2)$$

Where R is the ideal gas constant, and the activation energy E is also constant. But in some variants of this model the preexponential factor is a function of temperature in the form of the Equation 3:

$$A = A_0 T^m \quad (3)$$

Where A_0 is a constant ⁽¹³⁾. Integration of Eq. (2) with a constant heating rate β leads to Equation 4:

$$\int_0^\alpha \frac{d\alpha}{f(\alpha)} = \frac{A_0}{\beta} \left(\frac{E}{R}\right)^{m+1} [p_m(x) - p_m(x_0)] \quad (4)$$

Where Equation 5 is the *general* form of the temperature integral, being p a particular case of p_m with $m = 0$ and $A = A_0$.

$$p_m(x) = \int_x^\infty \chi^{-(m+2)} \exp(-\chi) d\chi \quad (5)$$

The integration variable χ is dimensionless, and the temperature defines the lower limit $x = E/RT$, but it implies that the limit $T_0 \rightarrow 0$ becomes $x \rightarrow \infty$. This indeterminate limit does not allow an analytical solution, but at the same time relates p_m with the special functions, as it will be explained in Section 4. On the other hand, the upper infinity limit is certainly an issue for the numerical integration of p_m , but it is solved in the next section.

For the comparisons between p_m values from formulas and from numerical integration in the following sections we chose $m = -3, -2.5, \dots, 0, \dots, 3$ because values of m between -1.5 and 2.5 in 0.5 increments have been reported for solid decomposition and gas-solid reactions ⁽¹³⁾. It is true that temperature-dependent preexponential factors are much less common than constant As, but our analysis of the general temperature integral covers $p(x)$ as the particular case $m = 0$, and $A = A_0$. Lower limit values were set as $x = 1, 2, 5, \dots, 100$ because x values in the interval [5,100] have been considered of practical significance ⁽¹⁴⁾.

3. Numerical integration

There are no sources of exact values for $p_m(x)$, it does not have analytical solution and even the

tables for $p(x)$ are rare, for example the Vallet compilation was published last in 1961 ^(1, 15, 16). However $p(x)$ reference values have been obtained by means of numerical integration, with the trapezoidal rule, or the integration routine included in the software Mathematica ⁽¹⁷⁻²⁰⁾.

In this work the reference values were also calculated by numerical integration the with the Simpson 3/8 rule. It was chosen as a compromise between accuracy and efficiency, after considering that for the same stepsize (h) the most intricate methods offer a better accuracy than the simple ones, but given that accuracy is inversely proportional to the stepsize, even simple methods can produce a very low error using a tiny h .

Following the Simpson 3/8 rule the temperature integral is approximated as the area sum (Equation 6):

$$p_m(x) = A_1 + A_2 + \dots + A_i + \dots \quad (6)$$

Where each term is calculated in a subinterval of length $3h$ with the Equation 7:

$$A_i = \frac{3h}{8} [f(\chi_{0,i}) + 3f(\chi_{1,i}) + 3f(\chi_{2,i}) + f(\chi_{3,i})] \quad (7)$$

Evaluating the argument of the integral, $f(\chi)$, at the points $\chi_{0,i} = x + 3(i-1)h$, $\chi_{1,i} = \chi_{0,i} + h$, $\chi_{2,i} = \chi_{0,i} + 2h$, and $\chi_{3,i} = \chi_{0,i} + 3h$ ^(21, 22).

It was also necessary to define the value of h , but the only guideline found in the literature was a temperature stepsize of $10^{-2}K$, which is useless as the integration variable is $x = E/RT$, not T ⁽¹⁹⁾. In order to choose a stepsize p_m s obtained with h values from 1 down to 10^{-5} were probed, finding that the averaged relative difference

(Figure 1) is less than 1% for any stepsize $h < 1$, and that the avgs were almost the same for $h = 10^{-4}$ and $h = 10^{-3}$. Although these results suggest that a stepsize of 0.001 is enough the reference values of $p_m(x)$ were calculated with a stricter value of $h = 10^{-5}$, which is much smaller than typical values of χ . The associated error in the Simpson 3/8 rule is $|(3h^5/80)f^{(4)}(\xi)| = 3.75 \times 10^{-27} \times |f^{(4)}(\xi)|$, where ξ is a value between the limits of integration ⁽²²⁾.

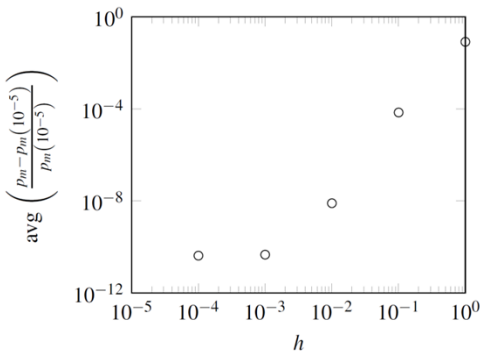


Figure 1. Averaged relative difference in $p_m(x)$ values respect to the reference result with $h = 10^{-5}$

Another issue in the numerical integration of Equations 1 and 5 arises from the representation of their infinity upper limits with some finite value, namely x_∞ . An apparently obvious choice for x_∞ is the biggest possible real number in the system, 1.79×10^{308} in the double precision 64 bit IEEE 754 standard ⁽²³⁻²⁵⁾, but it would require an unbearable long calculation time (a back of the envelope estimation for integration with the trapezoidal rule using $h = 1$ and $1\mu s$ per step yields 3×10^{294} years).

It was also considered defining x_∞ as the value such where the argument of the integral vanishes, that is $f(x_\infty) \approx 0 \approx \sigma$, where σ is the tiniest possible real number in the system ($\sigma = 4.94 \times 10^{-324}$ for double precision variables, standard IEEE 754). In this way, Equation 8:

$$\ln \sigma = -(m + 2) \ln(x_\infty) - x_\infty \quad (8)$$

And the results of solving this equation for $-3 \leq m \leq 3$ lead to $x_\infty = 750$. However, this hypothetical upper limit choice is computationally wasteful because for most of the A_i terms in Equation 6 the addition is irrelevant and unfeasible. It is illustrated here with an extreme example: using $h = 10^{-5}$ and $m = -3$ the result is $p_{-3}(100) = 3.76 \times 10^{-42}$, but the value of $A_i(\chi = 600)$ is 4.77×10^{-263} , and the following A_i s are even smaller.

Due to the order of magnitude difference, 10^{-42} vs. 10^{-263} , the addition of $A_i(\chi = 600)$ and the following A_i s does not alter the resulting value of p_m , it would only change its 221th and following digits, which are irrelevant in the sum. Moreover, these hundreds of digits do not exist, and are unnecessary, because the calculations of TGA data analysis is carried out with standard real variables of 15-17 decimal digits, which provide enough precision for the estimation of parameters (we emphasize that hypothetical number representations with hundreds of digits are *not* necessary for TGA data analysis).

A *static* upper limit x_∞ was discarded after considering the reasons in the previous paragraph, but Figure 2 shows that the integral argument in $p_m(x)$ decreases asymptotically to 0, suggesting to use the point where it becomes negligible as an equivalent to x_∞ .

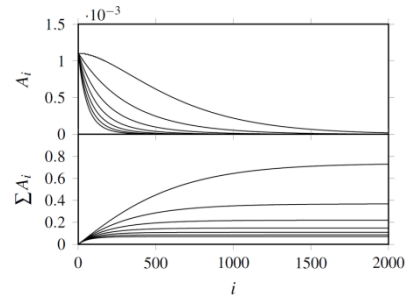


Figure 2. Areas from Simpson 3/8 rule integration (A_i , Eq.(7), upper half) and result $p_m(x) = \sum_1^i A_i$ (Eq.(6), lower half) as function of i . Results are shown for $m = -3, -2, \dots, 3$ with $x = 1$

In this way the area sum of Equation 6 is stopped in a dominant term, identified with the index i_∞

such that the subsequent terms do not numerically add to the result (Equation 9). Given that

$$p_m(x) = A_1 + A_2 + \dots + A_{i_\infty-1} + A_{i_\infty} + A_{i_\infty+1} + A_{i_\infty+2} + \dots$$

and

$$A_1 > A_2 > \dots > A_{i_\infty} > A_{i_\infty+1} > A_{i_\infty+2} > \dots \quad (9)$$

The calculation is stopped at A_{i_∞} and given that all subsequent areas are negligible results Equation 10

$$\sum_1^{i_\infty-1} A_i + \sum_{i_\infty}^{i_\infty-1} A_i = \sum_1^{i_\infty-1} A_i, \quad (10)$$

Then, dividing by $\sum_1^{i_\infty-1} A_i$ results Equation 11

$$1 + \sum_{i_\infty}^{i_\infty-1} A_i / \sum_1^{i_\infty-1} A_i = 1. \quad (11)$$

The index i_∞ is identified using the floating point arithmetic's machine epsilon, which is $\text{eps} = 2^{-52} \approx 2.220 \times 10^{-16}$ for 64 bit double precision variables ⁽²⁵⁾. It is the amount such that *numerically*

$$1 + \text{eps} = 1 \quad (12)$$

Hence, from the analogy between equations (11) and (12) i_∞ is the index i of the *first* A_i (Equation 13) such that

$$A_{i_\infty} / \sum_{i=1}^{i_\infty-1} A_i \leq \text{eps} \quad (13)$$

and the calculation is stopped when such condition is reached. Therefore, from Eq. (7) the equivalent upper integral limit is $x_\infty = \chi_{3,i_\infty}$, where i_∞ is the last term in the sum.

The use of i_∞ produced x_∞ values well below 750, as shown in Figure 3, and allowed to compute the temperature integrals in a reasonable time. For the same x (lower limit of

temperature integral), x_∞ decreases with the power m because it produces smaller $f(\chi)$ values, and the area sum reaches the point i_∞ where A_{i_∞} becomes insignificant with less terms. On the other hand, higher x values produce smaller initial A_i values and it is compensated with more terms for the sum $\sum_1^{i_\infty-1} A_i$ in Eq. (13), consequently x_∞ increases with x .

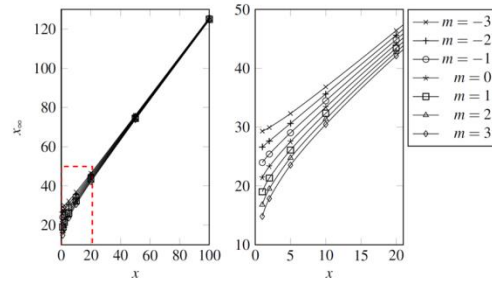


Figure 3. Upper limit, x_∞ for the integral p_m , calculated from i_∞ in Eq. (13). The right plot is a zoom of the area in the red rectangle. Results are shown for different m values

Evaluation of the temperature integral through numerical integration seems less efficient than the use of special functions, but it has not been extensively checked: in the only one comparison found in the literature the execution time of the trapezoidal rule integration is longer than in the Senum-Yang approximation by a factor of 10000 ⁽¹⁹⁾. However, numerical integration can be longer than necessary if the stepsize is too small (the number of evaluations is inversely proportional to h), albeit this minimize the implicit truncation error. In fact it was observed that even results obtained with $h \approx 1$ can have an acceptable accuracy. Due to this the effect of stepsize was analyzed comparing execution times from numerical integration and the incomplete gamma function (the representation of p_m in terms of Γ is explained in the next section), measured in the same computer, that is, with the same combination of hardware and

software, for $10^{-5} \leq h \leq 1$. The results in Figure 4 show that Simpson 3/8 integration requires more time than the incomplete gamma function, unless stepsize is close to 1.

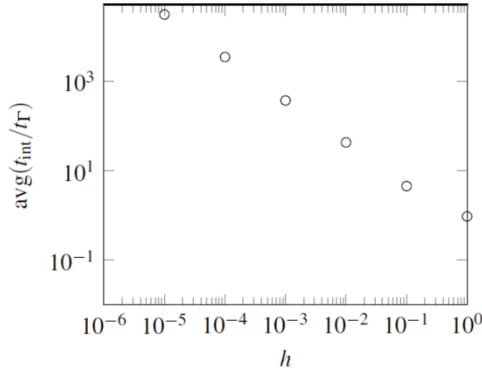


Figure 4. Averaged quotient of execution times (t , numerical integration) / (t , incomplete gamma function)

4. Calculation based on formulas

Despite the computational raw power available in current computers it is more practical to have a representation of $p(x)$ as a function than calculating it from numerical integration (in this work with Simpson 3/8 rule) each time it is required. However, the representations of $p(x)$ found in the literature have limitations. The series (Equation 14)

$$p(x) = \frac{e^{-x}}{x} + \gamma + \ln(x) + \sum_{n=1}^{\infty} \frac{(-1)^n x^n}{n \cdot n!}, \quad (14)$$

Where $\gamma = 0.5772156649 \dots$ is the Euler-Mascheroni constant, is valid for $x < \pi$ ^(15,26). In the same way the expansion in series of Bernoulli numbers (Equation 15)

$$p(x) = \frac{e^{-x}}{x^2} \left(-3.5 \times 10^{-6} + \frac{0.998710}{x} + \frac{1.984876}{x^2} + \dots \right), \quad (15)$$

Is valid for $x \leq 2$ ^(1,27). Multiple integration by parts generates the asymptotic expansion (Equation 16)

$$p(x) = \frac{e^{-x}}{x^2} \left(1 - \frac{2!}{x} + \frac{3!}{x^2} + \dots + \frac{(-1)^i (i+1)!}{x^i} + \dots \right), \quad (16)$$

But it is reliable only for large x values, namely $x > 20$ ^(1,15). The Schlömilch expansion (Equation 17)

$$p(x) = \frac{e^{-x}}{x(x+1)} \left(1 - \frac{1}{x+2} + \frac{1}{(x+2)(x+3)} - \frac{1}{(x+2) \dots (x+4)} + \dots \right), \quad (17)$$

Has been used occasionally to produce $p(x)$ tables, but it is limited and its results may not be precise ^(1, 15, 27, 28).

To overcome the limitations of the available $p(x)$ representations (Eq. 14-17) the values of the temperature integrals were rewritten in terms of the more common *special functions*: the exponential integrals E_1 and E_n ; and the incomplete gamma function, Γ . In this way $p(x)$ becomes in Equation 18 ⁽²⁹⁾

$$p(x) = \frac{e^{-x}}{x} - E_1(x) \quad (18)$$

While there are two possible forms for p_m (Equation 19):

$$p_m(x) = x^{-(m+1)} E_{m+2}(x) \quad (19)$$

And (Equation 20)

$$p_m(x) = \Gamma(-(m+1), x), \quad (20)$$

Which is a consequence of the special case (Equation 21) ⁽⁴⁾

$$E_n(x) = x^{n-1} \Gamma(1-n, x). \quad (21)$$

Moreover, the temperature integral $p(x)$ can also be written in terms of these p_m expressions, with $m = 0$

$$p(x) = x^{-1} E_2(x) = \Gamma(-1, x).$$

Special functions are defined in Equations 22, 23 and 24

$$E_1(x) = \int_x^\infty (e^{-t}/t)dt, \quad (22)$$

$$E_n(x) = \int_1^\infty t^{-n} \exp(-xt)dt, \quad (23)$$

$$\Gamma(a, x) = \int_x^\infty t^{a-1} e^{-t} dt. \quad (24)$$

The exponential integral E_1 was calculated with the common series expansion (Equation 25) ⁽³⁰⁻³²⁾

$$E_1(x) = -\left(\gamma + \ln x + \sum_{n=1}^\infty \frac{(-x)^n}{n \cdot n!}\right) \quad (25)$$

but in this work it was found that for $x > 10$ it results necessary to use the alternate divergent series form (Equation 26) ⁽³⁰⁾

$$E_1(x) = \frac{\exp(-x)}{x} \sum_{n=0}^{N-1} \frac{n!}{(-x)^n} \quad (26)$$

with $N = 15$ to obtain complete agreement with values tabulated in the *Handbook of Mathematical Functions* ⁽³²⁾. The incomplete gamma function was calculated with the continued fraction of the Equation 27

$$\Gamma(x, a) = e^{-x} x^a \left(\frac{1}{x+1} \frac{1-a}{1+x} \frac{1}{x+1} \frac{2-a}{1+x} \frac{2}{x+1} \dots \right), \quad (27)$$

using the Lentz algorithm ⁽²¹⁾. $\Gamma(a, x)$ was evaluated even with non-integer and negative values of a , and these results were checked with values from Wolfram's function site ⁽³³⁾. The numerical evaluation of $E_n(x)$ is very similar to the procedure for $\Gamma(a, x)$ because this exponential integral is a special case of the incomplete gamma function (Equation 28) ^(21, 31, 34)

$$E_n(x) = x^{n-1} \Gamma(1-n, x) \quad (28)$$

with

$$E_0(x) = \exp(-x)/x$$

and

$$E_n(0) = 1/(n-1).$$

In the general case with $0 \leq x \leq 1$ (Equation 29)

$$E_n(x) = \frac{(-x)^{n-1}}{(n-1)!} \left[-\ln(x) - \gamma + \sum_{r=1}^{n-1} \frac{1}{r} \right] - \sum_{\substack{r=0 \\ r \neq n-1}}^\infty \frac{(-x)^r}{(r-n+1)r!} \quad (29)$$

And the result if $x \approx > 1$ comes from the continued fraction in the Equation 30:

$$E_n(x) = e^{-x} \left(\frac{1}{x+n} \frac{n}{-x+n+2} \frac{2(n+1)}{-x+n+4} \dots \right). \quad (30)$$

As expected $p(x)$ results from $p_{m=0}(x)$, $x^{-1}E_2(x)$, and $\Gamma(-1, x)$ coincided, but a further comparison of $p_m(x)$ against numerical integration is presented in the following section.

5. Comparison

Temperature integral values from E_1 , E_2 , and Γ (see Section 4) were compared against the reference results defining the relative error as follows in the Equation 31:

$$\text{err} = \left| \frac{p_m(x) - p_{m,\text{intg}}(x)}{p_{m,\text{intg}}(x)} \right| \quad (31)$$

Where $p_{m,\text{intg}}$ is the reference value obtained from Simpson 3/8 numerical integration with $h = 10^{-5}$.

- For $p_m(x) = x^{-(m+1)} E_{m+2}(x)$ it was found that $\text{err} < 2 \times 10^{-10}$, except for $p_m(1)$ with $m = -3$ or $m = -2.5, \dots, -1.5, \dots, 2.5$. This is an effect of "forcing" noninteger or negative n values as arguments of the E_n function, which was originally conceived for integer n values with $n > 1$ (21).

- Results for $p_m(x)$ included $m = 0$, therefore $\text{err} < 2 \times 10^{-10}$ also for $p(x) = p_0(x) = x^{-1}E_2(x)$, for all x tested. Similar results were obtained for $p(x)$ calculated with E_1 except with $x = 10$ and $x = 20$. This suggests that it is preferable to evaluate $p(x)$ as $p_{m=0}(x) = x^{-1}E_2(x)$ to get a consistent relative error.

Results from incomplete gamma function, including $m = 0$, are summarized as follows:

- For $p_m(x) = \Gamma(-(m+1), x)$ $\text{err} < 2 \times 10^{-10}$ in all cases, including non-integer m values.
- Results from E_m and Γ produced very similar relative error values, except in the aforementioned case $p_m(1)$ with $m = -3$ or $m = -2.5, \dots, -1.5, \dots, 2.5$.

6. Conclusion

The temperature integral can be computed as $p_m(x) = \Gamma(-(m+1), x)$ for any m , integer or non-integer and $1 \leq x \leq 100$. Application of the exponential integral, E_{m+2} , is restricted to integer m values such that $m \geq -2$. The incomplete gamma function is preferable to the exponential integral because application of E_1 to calculate $p(x)$, although valid, can produce higher relative errors than the other two functions for high x values.

7. References

- (1) Flynn J. The 'Temperature Integral' — Its use and abuse. *Thermochim Acta* [Internet]. 1997;300(1–2):83–92. Available from: <https://www.sciencedirect.com/science/article/abs/pii/S0040603197000464>.
- (2) Galwey A. Is the science of thermal analysis kinetics based on solid foundations?: A literature appraisal. *Thermochim Acta* [Internet]. 2004;413(1–2):139–83. Doi: 10.1016/j.tca.2003.10.013. Available from: <https://www.sciencedirect.com/science/article/abs/pii/S0040603103005422?via%3Dihub>.
- (3) Órfão J. Review and evaluation of the approximations to the temperature integral. *AICHE J* [Internet]. 2007;53(11):2905–15. Doi: 10.1002/aic.11296. Available from: <https://aiche.onlinelibrary.wiley.com/doi/full/10.1002/aic.11296>.
- (4) Carrero J, Rojas A. A unified integral interpretation of thermal analysis data. *Ing y Compet* [Internet]. 2016;18(1):102–12. Available from: http://revistas.univalle.edu.co/index.php/ingenieria_y_competitividad/article/view/2181.
- (5) Vyazovkin S, Burnham A, Criado J, Pérez-Maqueda L, Popescu C, Sbirrazzuoli N. ICTAC Kinetics Committee recommendations for performing kinetic computations on thermal analysis data. *Thermochim Acta* [Internet]. 2011;520(1–2):1–19. Available from: <https://www.sciencedirect.com/science/article/pii/S0040603111002152>.
- (6) Vyazovkin S, Chrissafis K, Di Lorenzo M, Koga N, Pijolat M, Roduit B, et al. ICTAC Kinetics Committee recommendations for collecting experimental thermal analysis data for kinetic computations. *Thermochim Acta* [Internet]. 2014;590:1–23. Available from: <https://www.sciencedirect.com/science/article/pii/S0040603114002573>.
- (7) Portnyagin AS, Golikov AP, Drozd VA, Avramenko VA. An alternative approach to kinetic analysis of temperature-programmed reaction data. *RSC Adv*

- [Internet]. 2018;8(6):3286–95. Available from: <https://pubs.rsc.org/en/content/articlelanding/2018/ra/c7ra09848k#!divRelatedContent&articles>.
- (8) Hammam MAS, Abdel-Rahim MA, Hafiz MM, Abu-Sehly AA. New combination of non-isothermal kinetics-revealing methods. *J Therm Anal Calorim* [Internet]. 2017;128(3):1391–405. Available from: <https://link.springer.com/article/10.1007/s10973-017-6086-x>.
- (9) Holba P. Temperature dependence of activation energy of endothermic processes and related imperfections of non-isothermal kinetic evaluations. *J Therm Anal Calorim* [Internet]. 2017;129(1):609–14. Available from: <https://link.springer.com/article/10.1007/s10973-017-6088-8>.
- (10) Šesták J. The quandary aspects of non-isothermal kinetics beyond the ICTAC kinetic committee recommendations. *Thermochim Acta* [Internet]. 2015;611:26–35. Available from: <https://www.sciencedirect.com/science/article/pii/S0040603115001707>.
- (11) Šesták J. Are nonisothermal kinetics fearing historical Newton's cooling law, or are just afraid of inbuilt complications due to undesirable thermal inertia? *J Therm Anal Calorim* [Internet]. 2018;134(3):1385–93. Available from: <https://doi.org/10.1007/s10973-018-7705-x>.
- (12) Burnham AK. Use and misuse of logistic equations for modeling chemical kinetics. *J Therm Anal Calorim* [Internet]. 2017;127(1):1107–16. Available from: <https://link.springer.com/article/10.1007/s10973-015-4879-3>.
- (13) Criado J, Pérez-Maqueda LA, Sánchez-Jiménez PE. Dependence of the preexponential factor on temperature. *J Therm Anal Calorim* [Internet]. 2005;82(3):671–5. Available from: <https://link.springer.com/article/10.1007/s10973-005-0948-3>.
- (14) Deng C, Cai J, Liu R. Kinetic analysis of solid-state reactions: Evaluation of approximations to temperature integral and their applications. *Solid State Sci* [Internet]. 2009;11(8):1375–9. Available from: <http://dx.doi.org/10.1016/j.solidstatesciences.2009.04.009>.
- (15) Heal GR. Evaluation of the function $p(X)$, used in non-isothermal kinetics, by a series of Chebyshev polynomials. *Instrum Sci Technol* [Internet]. 1999;27(5):367–87. Available from: <https://www.tandfonline.com/doi/abs/10.1080/10739149908085873>.
- (16) Vallet P. Tables numériques permettant l'intégration des constantes de vitesse par rapport à la température [Internet]. Vol. 18, *Chemical Engineering Science*. Elsevier; 1961. 114 p. Available from: <https://www.sciencedirect.com/science/article/pii/000925096380007X>.
- (17) Cai J, Liu R. Dependence of the frequency factor on the temperature: A new integral method of nonisothermal kinetic analysis. *J Math Chem* [Internet]. 2008;43(2):637–46. Available from: <https://link.springer.com/article/10.1007/s10910-006-9215-5>.
- (18) Cai J, Wu W, Liu R. Isoconversional kinetic analysis of complex solid-state processes: Parallel and successive reactions. *Ind Eng Chem Res* [Internet]. 2012;51(49):16157–61. Available from: <https://pubs.acs.org/doi/abs/10.1021/ie302160d>.

- (19) Vyazovkin S, Dollimore D. Linear and nonlinear procedures in isoconversional computations of the activation energy of nonisothermal reactions in solids. *J Chem Inf Comput Sci* [Internet]. 1996;36(1):42–5. Available from: <https://pubs.acs.org/doi/abs/10.1021/ci950062m>.
- (20) Vyazovkin S, Wight CA. Estimating realistic confidence intervals for the activation energy determined from thermoanalytical measurements. *Anal Chem* [Internet]. 2000;72(14):3171–5. Available from: <https://pubs.acs.org/doi/abs/10.1021/ac000210u>.
- (21) Flannery BP, Teukolsky S, Press WH, Vetterling W. Numerical recipes in FORTRAN The art of scientific computing [Internet]. Second Edition. New York: Cambridge University Press; 1993. 933 p. Available from: <https://www.cambridge.org/es/academic/subjects/mathematics/numerical-recipes/numerical-recipes-fortran-example-book-art-scientific-computing?format=PB>.
- (22) Weisstein E. Simpson's 3/8 Rule [Internet]. Wolfram MathWorld. [Consulted 2018/12]. Available from: <http://mathworld.wolfram.com/Simpsons38Rule.html>.
- (23) Zuras D, Cowlishaw M. IEEE Standard for Floating-Point Arithmetic - Std 754™-2008 [Internet]. New York: IEEE Institute of Electrical and Electronics Engineers; 2008. 70 p. Doi: 10.1109/ieeestd.2008.4610935. Available from: https://ieeexplore.ieee.org/servlet/opac?pu_number=4610933.
- (24) Wikipedia. Double precision floating-point format [Internet] [Consulted in 2018/12]. Available from: https://en.wikipedia.org/wiki/Double-precision_floating-point_format.
- (25) Moler C. Floating Points MATLAB News and Notes [Internet]. 1996. Available from: https://www.mathworks.com/content/dam/mathworks/mathworks-dot-com/company/newsletters/news_notes/pdf/Fall96Cleve.pdf.
- (26) Senum G, Yang R. Rational approximations of the integral of the Arrhenius function. *J Therm Anal Calorim* [Internet]. 1977;11(3):445–7. Available from: <https://link.springer.com/article/10.1007/BF01903696>.
- (27) Flynn J, Wall LA. General treatment of the thermogravimetry of polymers. *J Res Natl Bur Stand* (1934) [Internet]. 1966;70a(6):487–524. Available from: https://nvlpubs.nist.gov/nistpubs/jres/70A/jresv70An6p487_A1b.pdf.
- (28) Zsakó J, Zsakó-Jr J. Kinetic analysis of thermogravimetric data. *J Therm Anal Calorim* [Internet]. 1980;19(2):333–45. Available from: <https://link.springer.com/article/10.1007/BF01915809>.
- (29) Farjas J, Roura P. Isoconversional analysis of solid state transformations A critical review. Part I. Single step transformations with constant activation energy. *J Therm Anal Calorim* [Internet]. 2011;105(3):757–66. Available from: <https://link.springer.com/article/10.1007/s10973-011-1446-4>.
- (30) Bleistein N, Handelsman RA. Asymptotic Expansions of Integrals. New York: Holt, Rinehart, and Winston; 1975. 425 p.
- (31) Cody W, Thacher HC. Rational Chebyshev Approximations for the

- Exponential Integral $E_1(x)$. Math Comput [Internet]. 1968;22(103):641–9. Available from: <https://www.ams.org/journals/mcom/1968-22-103/S0025-5718-1968-0226823-X/>.
- (32) Abramowitz M. Handbook of Mathematical Functions, With Formulas, Graphs, and Mathematical Tables. Washington, DC: National Bureau of Standards; 1964. 1046 p.
- (33) Wolfram Research I. Incomplete gamma function [Internet]. [Consulted 2018/12]. Available from: <http://functions.wolfram.com/GammaBetaErf/Gamma2/>.
- (34) Cody W, Thacher HC. Chebyshev Approximations for the Exponential Integral $E_1(x)$. Math Comput [Internet]. 1969;23(106):289–303. Available from: <https://www.ams.org/journals/mcom/1969-23-106/S0025-5718-1969-0242349-2/>.



Revista Ingeniería y Competitividad por Universidad del Valle se encuentra bajo una licencia Creative Commons Reconocimiento - Debe reconocer adecuadamente la autoría, proporcionar un enlace a la licencia e indicar si se han realizado cambios. Puede hacerlo de cualquier manera razonable, pero no de una manera que sugiera que tiene el apoyo del licenciador o lo recibe por el uso que hace.